Bioconjugate Chemistry

Article

pubs.acs.org/bc

Investigating Hapten Clustering as a Strategy to Enhance Vaccines against Drugs of Abuse

Karen C. Collins and Kim D. Janda*

Departments of Chemistry and Immunology, The Skaggs Institute for Chemical Biology, Worm Institute of Research and Medicine (WIRM), The Scripps Research Institute, 10550 North Torrey Pines Road, La Jolla, California 92037, United States

Supporting Information

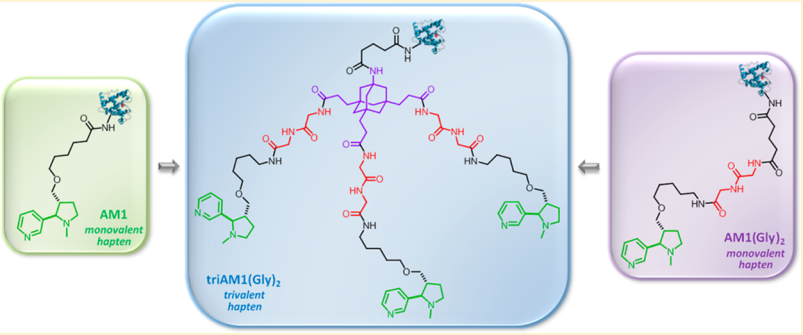

ABSTRACT: Vaccines for drugs of abuse have yet to achieve full clinical relevance, largely due to poor/inconsistent immune responses in patients. The use of multivalent scaffolding as a means to tailor drug−hapten density and clustering was examined in the context of drug-immune response modulation. A modular trivalent hapten containing a diglycine spacer, triAM1$(Gly)_2$, was synthesized and shown to elicit anti-nicotine antibodies at equivalent affinity and concentration to the monovalent AM1 analog, despite in this instance having a lower effective hapten density. Augmenting this data, the corresponding monovalent hapten AM1$(Gly)_2$ resulted in enhanced antibody affinity and concentration. Drug-hapten clustering represents a new vaccine paradigm, and, while examined only in the context of nicotine, it should be readily translatable to other drugs of abuse.

INTRODUCTION

Smoking is the leading cause of preventable death and illness worldwide, with over 5 million tobacco-related deaths reported annually.[1] Unassisted attempts to quit smoking have a poor success rate, and although current medications (including nicotine replacement, nicotine receptor agonists, antidepressants, and counseling) increase short-term cessation, improved therapies to increase long-term abstinence are required.[2] A therapeutic strategy currently in clinical development is vaccination against nicotine, where anti-nicotine antibodies are generated that can sequester the stimulant, preventing it from binding to nicotinic acetylcholine receptors in the brain. In theory, this approach would negate the positive feedback requisite for addiction and relapse. However, vaccines against nicotine have so far shown limited efficacy as antibody responses have proven highly variable, and only the small percentage of individuals who sustained high anti-nicotine antibody titers remained abstinent over the long term.[3,4] These findings do however validate the approach, and development of a vaccine that gives consistently high titers in a non-population-specific manner should provide significant improvement to long-term smoking cessation success rates.

Small molecules cannot themselves elicit an immune response, and need to be covalently attached to a protein or peptide to enable recognition by the immune system.[5] The carrier serves two purposes: first, it presents multiple copies of the small molecule hapten to B cells, which are then activated upon cross-linking of their B cell receptors (BCRs). Second, in order for the immune response to be specific, fervent, and long-lasting, isotype switching from IgM to IgG needs to be promoted by coactivation of T cells. However, T cell activation can only occur through presentation of *peptidic* fragments on the major histocompatibility complex (MHC) of an antigen presenting cell. It has also been observed that increasing the copies of hapten conjugated to the carrier protein surface (hapten density) is generally correlated with an increase in immune response strength and specificity,[6] although it should be noted that excessive BCR cross-linking has been observed to result in B cell anergy.[5]

We posited that through the use of hapten clustering the immune response would be enhanced by facilitating an increase in the maximum potential (effective) hapten density on the protein carrier, creating a higher avidity interaction with the B cell and in theory promoting increased cross-linking of the BCRs through the colocalization of multiple hapten copies. Although the optimal spatial distribution of the hapten is still

Received: January 11, 2014
Revised: February 7, 2014
Published: February 12, 2014

   dx.doi.org/10.1021/bc500016k | *Bioconjugate Chem.* 2014, 25, 593−600

unknown, it has been demonstrated that a hapten spacing of 5−10 nm with a hapten density of at least 10−20 per carrier resulted in robust B cell activation,[7] an achievable goal for a small molecule hapten display.

Hapten clustering has been extensively investigated in the field of carbohydrate vaccines, where this approach is thought to enhance the immune response by mimicking the natural spatial arrangement of carbohydrates on cancer cells, while also promoting more efficient B cell receptor cross-linking.[8,9] Existing methods to achieve hapten clustering primarily consist of hapten display on linear, cyclic, and dendrimeric peptidic scaffolds (e.g., RAFTs[10,11] and MAPs[12]). This approach is well-suited to carbohydrate vaccines where antibody production to the entire cluster may be an advantage, but this is not the case for small molecules, and the only example of application to drugs of abuse was a divalent attachment to a linear peptide, where the monovalent counterpart was more effective.[13] As an alternative approach to increase the hapten density within the drugs of abuse vaccine arena, we envisaged the use of a small molecular scaffold containing a core that would allow diverging three-dimensional projection of the hapten copies to promote spatial separation.

With this in mind, we wished to pursue a comparative study to investigate the use of different hapten display methods, wherein the absolute efficacy should not alter the findings and any results should be translatable to other haptens engaged in vaccines against drugs of abuse. For this purpose, we selected our readily accessible 3′-substituted nicotine-hapten, AM1, **1**;[14−16] this hapten-linker regiochemical display has been used in the majority of nicotine vaccines that have progressed furthest through clinical trials, with both NicVAX[3] (Cytos Biotechnology) and NicQβ[4] (Nabi Pharmaceuticals) using 3′ conjugates of nicotine (Figure 1). However, 3′-AmNic has

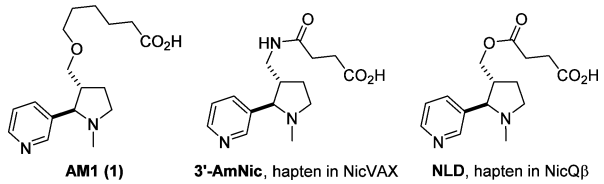

Figure 1. Structures of AM1 (**1**) and haptens used in NicVAX and NicQβ.

subsequently been shown to elicit antibodies with poorer nicotine affinities than other hapten-linker presentations.[17] In addition, we switched our choice of carrier protein from keyhole limpet hemocyanin (KLH) to ovalbumin (OVA), which although less immunogenic[18,19] has the benefit of allowing direct measurement of hapten incorporation by MALDI-TOF MS, as hapten density was a fundamental variable in our comparative study.

To summarize, we envisaged that the sequence of events that would culminate in an unique multihaptenic display could be enabled through the use of a synthetic scaffold that was immunogenically silent, and would allow for effective three-dimensional projection of the hapten cluster to achieve recognition of the monomer while simultaneously effecting cross-linking of the BCRs. Adamantane has been used as a scaffold core for numerous applications,[20] and is also a component of small molecule drugs for a wide range of indications.[21] Trifunctionalization of its C4 symmetric scaffold with the hapten at three vertices, leaving the fourth available for attachment to the carrier protein, would result in the display of a trihaptenic cluster, simultaneously tripling the potential hapten density. While the scaffold allows rigid three-dimensional projection of the cluster, well-chosen linkers introduce flexibility; this combination should facilitate recognition of individual monomeric units. Finally, late-stage introduction of the hapten allows for a divergent, yet modular, approach toward optimization of the system.

RESULTS AND DISCUSSION

We began by synthesizing the required nicotine−hapten scaffold appendages thus: alcohol **2** was prepared according to the literature in 2 steps from cotinine,[23] and then this was transformed into AM1 (**1**) as previously reported,[14] in high overall yield (Scheme 1). The corresponding AM1-NH_2 **4** was synthesized in an analogous manner from alcohol **2** by reaction with 5-bromovaleronitrile and reduction of the intermediate nitrile **3** in moderate yield. The required decoration of the adamantane scaffold could be achieved on gram scale following previous methods,[24−27] and the introduction of a 5-carbon linker gave triacid **6**. Subsequent coupling with AM1-NH_2 **4** and ester hydrolysis gave triAM1 (**7**) in good yield.

Next, AM1 and triAM1 were activated with sulfo-NHS and conjugated to OVA. Conjugation efficiency of triAM1 (2.75 ≡ 8.24 copies of nicotine−hapten) was significantly lower than AM1 (11.4 copies), as determined by MALDI-TOF, likely a result of the use of a comparatively smaller molar excess, as well as a possible cumulative negative impact of the conjugation of this large molecule on successive reactions of surface lysines. Nevertheless, these conjugates were formulated with SAS and the efficacies of the vaccines determined by vaccination of BALB/c mice (n = 6). The obtained plasma antibody titers were determined by ELISA (Figure 2). Titers for bleeds at days 42 and 56 from mice vaccinated with AM1-OVA were significantly higher than those vaccinated with triAM1-OVA, with no increasing immune response apparent for the latter conjugate throughout the study.

To further evaluate this scaffold strategy, RIA was used to gauge the immune response. While the traditional mindset has been to use ELISA as the metric to judge hapten−antibody immune response, this methodology grossly misrepresents the true immune response to small molecule antigens since the affinity and avidity of the antibodies to a solid-supported hapten-protein conjugate is not representative of the interaction with the soluble hapten.[32] Initial experiments to determine plasma antibody concentrations that could bind the L-(−)-[*N*-methyl-^{3}H]-nicotine tracer supported the significantly poorer immune response elicited by the triAM1 hapten; plasma taken from triAM1-OVA vaccinated mice at day 56 could only bind ca. 12% tracer at the highest achievable concentration, compared with ca. 44% binding for half this concentration of plasma elicited by AM1-OVA. Therefore, further analysis was not attempted.

The poor immunogenicity of triAM1 as a hapten could partially be attributed to the lower hapten density on the carrier protein compared with AM1, although this was thought unlikely to account for the entire disparity. The lower immunogenicity of this trivalent hapten is comparable to a finding in a recent study by Sanderson, where a peptidic, monovalent vaccine against methamphetamine showed a greater immune response than the corresponding divalent vaccine, with two identical haptens appended to both amines of the *N*-terminal lysine residue.[13] Further analysis of the mouse

dx.doi.org/10.1021/bc500016k | *Bioconjugate Chem.* 2014, 25, 593−600

Scheme 1. Synthesis of AM1 (1) and triAM1 (7)

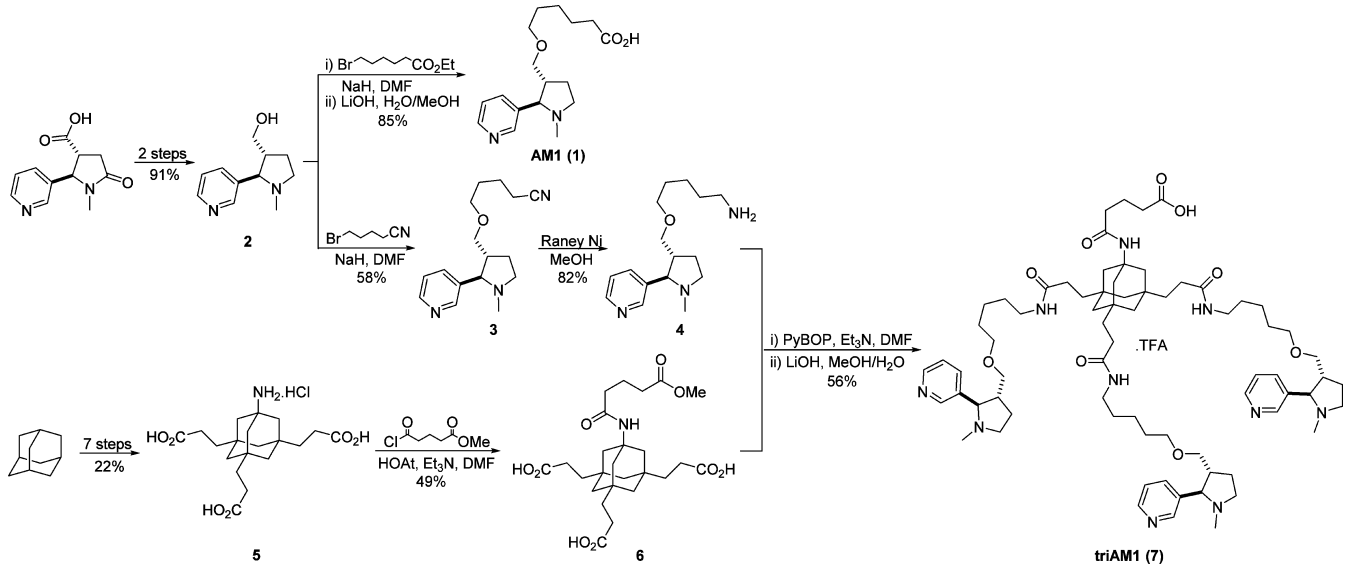

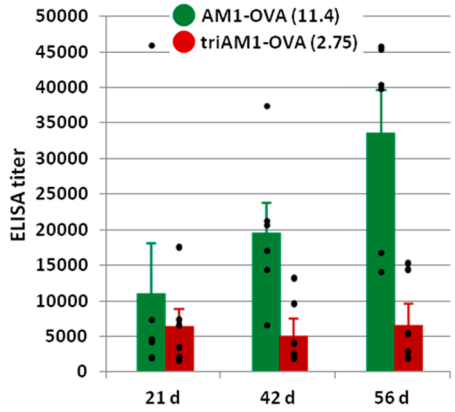

Figure 2. Midpoint antibody titers from AM1-OVA and triAM1-OVA vaccinated mice (n = 5–6) as determined by ELISA using AM1-BSA as the coating antigen. Data were obtained in duplicate. Numbers in parentheses represent the hapten density; error bars represent standard error of the mean (SEM); individual points represent individual mouse titers.

plasma showed that antibodies raised against triAM1-OVA had a substantially increased response to triAM1-BSA coated ELISA plates (Figure S1, Supporting Information), suggesting that recognition of the monomer is not being achieved; hence, the display may be too "dense" to allow for antibody production to a single copy of AM1, resulting in the production of antibodies that have poor affinity for nicotine. Additionally, this compact display may not allow simultaneous binding to multiple BCRs, preventing the cluster from efficiently effecting B cell stimulation. However, there was significant variability in antibody titers within both groups of mice, and two of the mice vaccinated with triAM1-OVA produced antibodies with titers as high as 15 000 at 56 d (Figure 2, Supporting Information), suggesting that it is possible for this drug–hapten scaffold to elicit a moderate immune response in a subset of the population.

Having established a lower limit benchmark of our adamantane hapten cluster, it was hoped that optimization of the hapten's linker would result in more effective recognition of the monomer as well as increased BCR cross-linking and thus an enhanced immune response in a higher percentage of mice. As a second generation candidate, we chose to introduce a short polyglycine spacer between the hapten and the scaffold, as this has previously been used in vaccination against oxycodone, where it was found to enhance the immunogenicity of the hapten, giving higher titers than a similar vaccine without the tetraglycine unit (although it must be noted that there was simultaneous alteration of the hapten itself, which may have effected some or all of the higher immune response).[33] The new target, triAM1$(Gly)_2$ (**10**), thus contained all the elements of triAM1 (**7**), with the addition of diglycine spacers between the adamantane scaffold and the three hapten copies (Scheme 2). Synthesis was achieved by the introduction of the diglycine unit onto AM1-NH_2, **4**; Boc-deprotection of carbamate **8** followed by coupling to the scaffold and subsequent ester hydrolysis gave the target in good yield. In an attempt to delineate modification of the hapten from the cluster effect, we also investigated incorporation of the diglycine unit into the monovalent hapten. Therefore, the same linker as appended to the scaffold for conjugation to the protein was coupled to diamide **9** to afford AM1$(Gly)_2$ (**11**) in moderate yield. Again, conjugation to OVA of the trivalent scaffold, in this case triAM1$(Gly)_2$, gave a far lower conjugation efficiency (1.98 ≡ 5.93 copies of nicotine hapten) than AM1$(Gly)_2$ (5.79 copies) with both achieving a lower (effective) hapten density than AM1 (10.6 copies).

Following immunization of mice using the OVA-conjugates, AM1-OVA was found to elicit similar titers to the conjugate from the first round of vaccinations as well as a similar pattern of variation between the mice within the group, as expected given that both conjugates had similar hapten densities (study 1: 11.4 copies, titer of 33 518; study 2: 10.6 copies, titer of 54 755). Although quantitative comparison of these titers would be inappropriate given that they were performed separately, the qualitative similarity in the titers obtained served to validate the reproducibility of this vaccination protocol.

Within the new study, comparable titers for all three conjugates was observed, which was exciting given the lower hapten densities of both of triAM1$(Gly)_2$ and AM1$(Gly)_2$ compared to AM1 (Figure 3). Furthermore, the variability of titers within the triAM1$(Gly)_2$-OVA group was much lower

dx.doi.org/10.1021/bc500016k | *Bioconjugate Chem.* 2014, 25, 593–600

Scheme 2. Synthesis of triAM1(Gly)$_2$ (10) and AM1(Gly)$_2$ (11)

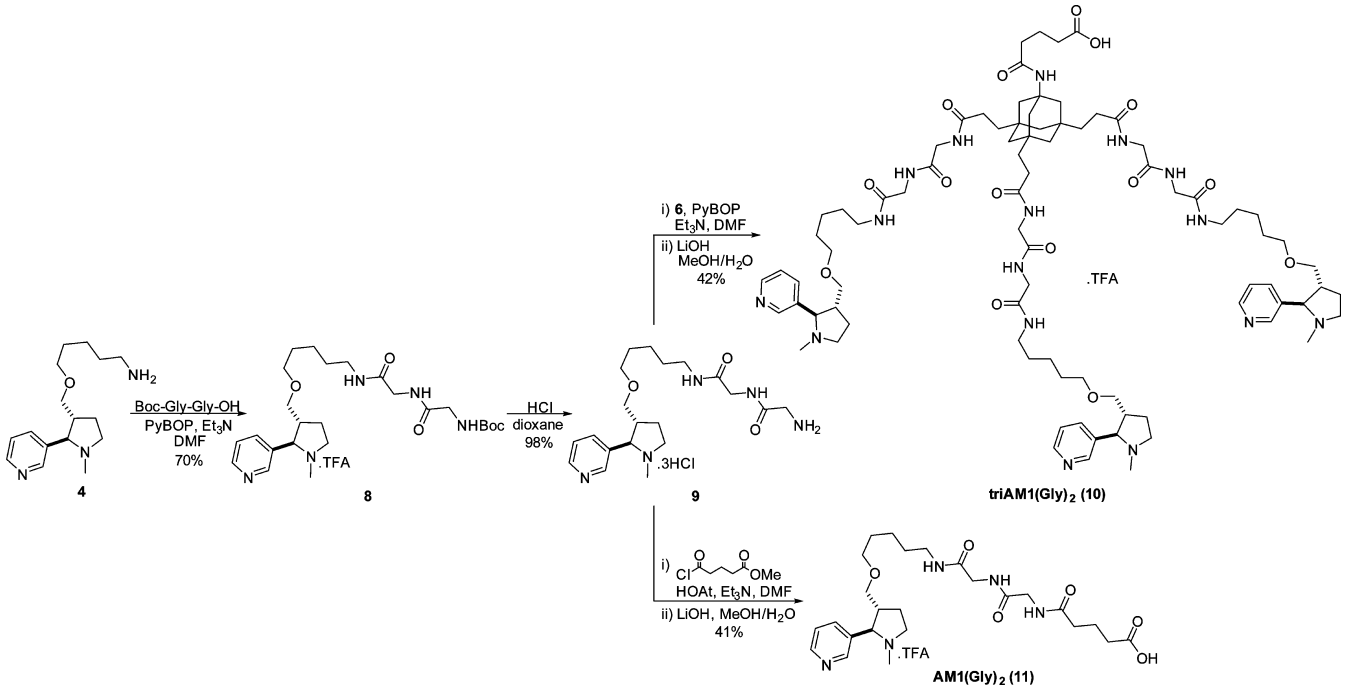

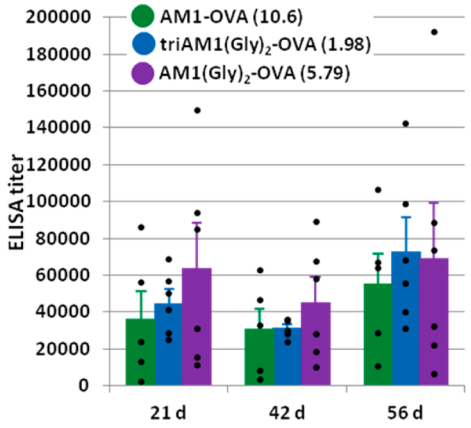

Figure 3. Midpoint antibody titers from AM1-OVA, triAM1(Gly)$_2$-OVA, and AM1(Gly)$_2$-OVA vaccinated mice (n = 5−6) as determined by ELISA using AM1-BSA as the coating antigen. Data were obtained in duplicate. Numbers in parentheses represent the hapten density, error bars represent SEM, individual points represent individual mouse titers.

than was seen for the monovalent hapten groups, with none of the mice in this group exhibiting poor anti-nicotine titers.

In order to determine the antibody specificity for the monovalent hapten over the trivalent hapten, ELISAs were also carried out using both triAM1(Gly)$_2$-BSA and AM1(Gly)$_2$-BSA as the coating antigens (Figure S2, Supporting Information). TriAM1-OVA had previously demonstrated enhanced recognition of the trivalent hapten over the monovalent hapten (Figure S1, Supporting Information). However, this effect was significantly reduced for triAM1(Gly)$_2$, which gave an improved selectivity profile toward the monovalent hapten. This suggests that we were correct in our hypothesis that the introduction of the peptidic linker favored the recognition of the monomeric hapten. Unsurprisingly, no significant difference was observed between titers of any group with AM1-BSA and AM1(Gly)$_2$-BSA as the coating antigens. On the basis of these promising results, we would suggest that nicotine−hapten clustering could provide a path forward to obtain more consistent immune responses across the population, something that has been strongly lacking in previous nicotine vaccines.[3,4]

RIA analysis supported the efficacy of the multihaptenic display; triAM1(Gly)$_2$-OVA elicited very similar antibody affinity and concentration (155 nM, 38.4 μg/mL) to AM1-OVA (167 nM, 45.9 μg/mL) at day 56, even at a lower effective hapten density, suggesting that the immune system is able to successfully recognize the monohapten units (Table 1). Moreover, a hapten density as low as 1.98 copies per carrier would likely only elicit a poor immune response, supporting our hypothesis that clusters can increase the effective hapten density and contribute to B cell activation. In turn, AM1(Gly)$_2$-OVA elicited much higher antibody affinity and concentration

Table 1. Anti-Nicotine Antibody Affinities and Concentrations from AM1-OVA, triAM1(Gly)$_2$-OVA, and AM1(Gly)$_2$-OVA Vaccinated Mice (n = 5−6) Using Pooled Plasma (56 d) as Determined by Competitive RIA[a]

Vaccine	Copies per OVA molecule	K_d[b] (nM)	Antibody concentration[b] (μg/mL)
AM1-OVA	10.6	167 ± 2.79 **	45.9 ± 2.39 **
triAM1(Gly)$_2$-OVA	1.98 (≡5.93)	155 ± 23.0 #	38.4 ± 7.92 #
AM1(Gly)$_2$-OVA	5.79	82.2 ± 13.1 **,#	82.1 ± 8.53 **,#

[a]Data for AM1(Gly)$_2$ were obtained in triplicate, and data for AM1 and triAM1(Gly)$_2$ were obtained in duplicate. Errors represent SEM. [b]Differences between values with matching symbols within a column are statistically significant (#p < 0.05, **p < 0.01).

dx.doi.org/10.1021/bc500016k | Bioconjugate Chem. 2014, 25, 593−600

(82.2 nM, 82.1 μg/mL) than AM1-OVA, suggesting that the presence of the polyglycine linker significantly enhances the immune response.[33] The hapten density in this case is again lower than that of AM1, which suggests that this vaccine compares even more favorably than these results show. A direct comparison of triAM1$(Gly)_2$-OVA and AM1$(Gly)_2$-OVA, which possess very similar effective hapten densities, leads us to posit that the trivalent scaffold will require additional "retooling" wherein optimization of the peptidic linker and protein conjugation chemistry will be required, the goal being to achieve the postulated antibody concentration (200 μg/mL[34]) required for a successful clinical candidate. However, having in this study established the powerful underlying logic of drug−hapten clustering with an ability to display as much as triple the effective hapten density, we surmise that such a recourse could yield a highly effective vaccine.

CONCLUSION

We have presented new insights into several factors that can greatly impact drug immunogenicity: hapten clustering, density, linker length, and its peptidic constitution. While further optimization for each of these components will be needed, our modular synthetic assembly, which will allow for efficient iterative improvement of each of these variables, is noteworthy. Importantly, this modular design should readily translate to the targeting of any desired drug of abuse. Key findings from our study are: (1) that a unique hapten cluster, triAM1$(Gly)_2$, was found to elicit a robust immune response that parallels that of a monovalent display, AM1, despite its lower effective hapten density; (2) the intermouse variability in the immune response for this hapten cluster was remarkably diminished in comparison to both monovalent haptens, AM1 and AM1-$(Gly)_2$, a major issue that has plagued drug abuse vaccines that have advanced to clinical trials. Finally, it is anticipated that upon optimization of the conjugation chemistry, increased immunogenicity will be seen with continued limiting of subject variability.

EXPERIMENTAL SECTION

Reactions were carried out under an argon atmosphere at rt using flame-dried glassware with dry solvents, and reagents were used as commercially supplied, unless otherwise specified. ^1H and ^{13}C NMR were performed on Bruker and Varian spectrometers, with the reference from the residual solvent peak for ^1H NMR (7.26 ppm for $CDCl_3$, 3.31 ppm for CD_3OD), and the solvent peak for ^{13}C NMR (77.1 ppm for $CDCl_3$, 49.0 ppm for CD_3OD). RP-HPLC was performed on an Agilent Technologies 1260 Infinity system using a Grace Vydac C18 column, 10−15 μm, 250 × 22 mm using method 1: [A = 0.1% TFA/H_2O, B = 0.1% TFA/MeCN; λ = 254 and 210 nm; gradient 1% B (5 min), 1−15% B (15 min), 15−95% B (25 min), 95% B (5 min)]; or method 2: [gradient 1% B (5 min), 1−15% B (15 min), 15−75% B (35 min), 75−95% B (10 min), 95% B (5 min)]. Flash chromatography was performed on silica gel (SiliaFlash P60 40−63 μm, 230−400 mesh) according to the method of W. C. Still.[22] TLC was performed on glass-backed plates precoated with silica (EMD 60 F_{254}, 0.25−1 mm) and developed using standard visualizing agents: UV fluorescence (254 nm) and $KMnO_4$, cerium ammonium nitrate, or ninhydrin with appropriate heating. HRMS (ESI) were performed on an Agilent 1100 Series LC/MSD-TOF.

(*trans*-1-Methyl-2-(pyridin-3-yl)pyrrolidin-3-yl)-methanol, 2. This was synthesized in 2 steps from *trans*-4-cotininecarboxylic acid according to the method of Castagnoli.[23]

6-((*trans*-1-Methyl-2-(pyridin-3-yl)pyrrolidin-3-yl)-methoxy)hexanoic acid, AM1, 1. This was synthesized from alcohol **2** and ethyl 6-((methylsulfonyl)oxy)hexanoate according to the method of Janda.[14,15]

5-((*trans*-1-Methyl-2-(pyridin-3-yl)pyrrolidin-3-yl)-methoxy)pentanenitrile, 3. DMF (15 mL) was added to a mixture of alcohol **2** (630 mg, 3.28 mmol) and NaH (236 mg, 9.83 mmol) at 0 °C and the solution stirred (20 min), whereupon 5-bromovaleronitrile (574 μL, 4.92 mmol) was added and the solution allowed to slowly warm to rt and stirred (19 h). The solution was cooled to 0 °C and the reaction quenched with H_2O (350 μL) before the solvent was removed in vacuo. Purification by column chromatography eluting with MeOH/CH_2Cl_2 (gradient, 0:1 → 1:9) gave the title compound as a pale yellow oil (522 mg, 58%), R_f 0.54 (1:9 MeOH/CH_2Cl_2); δ_H ($CDCl_3$, 600 MHz) 8.51−8.47 (2H, m), 7.69 (1H, d, J = 7.7 Hz), 7.27−7.24 (1H, m), 3.37−3.30 (4H, m), 3.20 (1H, t, J = 8.6 Hz), 2.83 (1H, d, J = 8.3 Hz), 2.35−2.26 (4H, m), 2.16−2.10 (4H, m), 1.64−1.59 (5H, m); δ_C ($CDCl_3$, 151 MHz) 150.1, 148.9, 138.0, 135.3, 123.7, 119.8, 72.8, 72.5, 69.9, 56.1, 48.1, 40.5, 28.6, 27.0, 22.6, 17.1; HRMS (ESI): m/z calc'd for $C_{16}H_{24}N_3O$ $[MH]^+$ 274.1914, found 274.1927.

5-((*trans*-1-Methyl-2-(pyridin-3-yl)pyrrolidin-3-yl)-methoxy)pentan-1-amine, 4. A slurry of activated Raney nickel in H_2O (8 mL) was added to a solution of nitrile **3** (465 mg, 1.70 mmol) in MeOH (16 mL) at rt, and stirred under an H_2 atmosphere (1.5 h), whereupon the reaction mixture was filtered through Celite, washing with MeOH. The solvent was removed in vacuo to give the title compound as a pale yellow oil (387 mg, 82%), δ_H (CD_3OD, 500 MHz) 8.50 (1H, s), 8.45 (1H, d, J = 4.8 Hz), 7.86 (1H, d, J = 7.7 Hz), 7.46−7.40 (1H, m), 3.62−3.58 (2H, m), 3.42−3.37 (2H, m), 3.37−3.31 (2H, m), 3.20 (1H, t, J = 8.8 Hz), 3.05−2.97 (2H, m), 2.59 (1H, t, J = 7.3 Hz), 2.43−2.31 (2H, m), 2.18−2.10 (4H, m), 1.72−1.63 (1H, m), 1.52−1.38 (4H, m), 1.33−1.23 (2H, m); δ_C ($CDCl_3$, 126 MHz) 150.1, 148.8, 138.3, 135.3, 123.6, 72.7, 72.4, 71.1, 56.1, 48.2, 42.2, 40.5, 33.6, 29.5, 27.2, 23.6; HRMS (ESI): m/z calc'd for $C_{16}H_{28}N_3O$ $[MH]^+$ 278.2227, found 278.2228.

3,3′,3″-(7-Aminoadamantane-1,3,5-triyl)tripropionic Acid, 5. This was synthesized from adamantane in 7 steps according to the methods of Delimarskii, Baum, and Maison.[24−27]

3,3′,3″-(7-(5-Methoxy-5-oxopentanamido)-adamantane-1,3,5-triyl)tripropanoic Acid, 6. Et_3N (138 μL, 0.990 mmol) was added to a solution of HOAt (57 mg, 0.421 mmol) in DMF (2 mL) at 0 °C and the solution stirred (10 min) before the addition of methyl 5-chloro-5-oxovalerate (41 μL, 0.297 mmol) and the solution stirred at rt (1.5 h). This solution was then added dropwise to a solution of amine **5** (100 mg, 0.248 mmol) in DMF (3 mL) at 0 °C and stirred (18 h), whereupon H_2O (400 μL) was added, and the solution stirred (10 min) before the solvent was removed in vacuo. Purification by preparative RP-HPLC (method 1, R_t = 33.5 min) followed by lyophilization gave the title compound as a colorless oil (60 mg, 49%), δ_H (CD_3OD, 600 MHz) 3.66 (3H, s), 3.65 (1H, s), 2.34 (2H, t, J = 7.4 Hz), 2.33−2.25 (6H, m), 2.15 (2H, t, J = 7.3 Hz), 1.86 (2H, p, J = 7.3 Hz), 1.66−1.61 (6H, m), 1.55−1.50 (6H, m), 1.21−1.16 (3H, m), 1.14−1.08 (3H, m); δ_C (CD_3OD, 151 MHz, mixture of rotamers and/or salt forms)

dx.doi.org/10.1021/bc500016k | Bioconjugate Chem. 2014, 25, 593−600

178.1, 178.1, 176.4, 176.4, 175.3, 174.7, 54.8, 54.8, 52.1, 52.1, 46.2, 46.2, 45.6, 45.5, 39.0, 39.0, 38.9, 38.9, 36.8, 35.9, 33.9, 29.0, 28.9, 22.3; HRMS (ESI): m/z calc'd for $C_{25}H_{37}NO_9Na$ $[MNa]^+$ 518.2360, found 518.2363.

5-Oxo-5-((3,5,7-tris(3-((*trans*-5-((-1-methyl-2-(pyridin-3-yl)pyrrolidin-3-yl)methoxy)pentyl)amino)-3-oxopropyl)adamantan-1-yl)amino)pentanoic acid, triAM1, 7. PyBOP (126 mg, 0.242 mmol) and Et_3N (68 μL, 0.484 mmol) were added to a solution of triacid **6** (30 mg, 0.0605 mmol) in DMF (1 mL) and the solution stirred at rt (20 min) before the addition of a solution of amine **4** (67 mg, 0.242 mmol) in DMF (2 mL) and the solution stirred at rt (5 min). The reaction was quenched with H_2O (20 μL) and stirred at rt (5 min) before the solvent was removed in vacuo. Partial purification by preparative RP-HPLC (method 2, R_t = 33.4 min) followed by lyophilization gave the intermediate ester as a pale yellow oil. This was dissolved in MeOH (1 mL), 4 M aq. LiOH (150 μL) was added and the reaction stirred at rt (18 h). Purification by preparative RP-HPLC (method 2, R_t = 32.7 min) followed by lyophilization gave the title compound as a pale yellow oil (43 mg, 56%), δ_H (CD_3OD, 500 MHz) 8.92 (3H, s), 8.82 (3H, d, J = 4.2 Hz), 8.44 (3H, d, J = 7.5 Hz), 7.89−7.84 (3H, m), 4.46 (3H, br d, J = 9.0 Hz), 3.92 (3H, br s), 3.57−3.46 (6H, m), 3.44−3.36 (3H, m), 3.36−3.31 (6H, m), 3.10 (6H, t, J = 7.1 Hz), 3.07−2.99 (3H, m), 2.83 (9H, s), 2.48−2.39 (3H, m), 2.36−2.24 (3H, m), 2.20−2.08 (12H, m), 1.84 (2H, p, J = 7.5 Hz), 1.65 (6H, s), 1.52−1.47 (6H, m), 1.45−1.37 (12H, m), 1.22−1.14 (9H, m), 1.11 (3H, d, J = 12.1 Hz); δ_C (CD_3OD, 151 MHz, mixture of rotamers and/or salt forms) 176.8, 176.6, 174.8, 162.2 (q, $J(^{13}C-^{19}F)$ 36.1), 148.6, 148.3, 142.7, 132.3, 127.3, 117.7 (q, $J(^{13}C-^{19}F)$ 290.7), 73.2, 72.0, 71.2, 62.7, 56.7, 54.9, 52.1, 46.5, 45.6, 40.4, 40.3, 40.2, 39.1, 37.0, 36.8, 36.1, 35.9, 34.1, 33.9, 33.2, 31.2, 30.1, 30.1, 26.0, 24.5, 24.3, 22.5, 22.4; HRMS (ESI): m/z calc'd for $C_{72}H_{111}N_{10}O_9$ $[MH]^+$ 1259.8530, found 1259.8536.

***tert*-Butyl (2-((2-((5-((*trans*-1-methyl-2-(pyridin-3-yl)-pyrrolidin-3-yl)methoxy)pentyl)amino)-2-oxoethyl)-amino)-2-oxoethyl)carbamate, 8.** PyBOP (281 mg, 0.541 mmol), Et_3N (226 μL, 1.62 mmol), and amine **4** (100 mg, 0.360 mmol) were added to a solution of Boc-Gly-Gly-OH (126 mg, 0.541 mmol) in DMF (2.5 mL) and the solution was stirred at rt (30 min). The reaction was quenched with H_2O (20 μL) and the reaction stirred at rt (5 min) before the solvent was removed in vacuo. Purification by preparative RP-HPLC (method 2, R_t = 32.3 min) followed by lyophilization gave the title compound as a colorless oil (152 mg, 70%), δ_H (CD_3OD, 600 MHz) 8.97 (1H, s), 8.86 (1H, d, J = 5.0 Hz), 8.52 (1H, d, J = 7.8 Hz), 7.94 (1H, dd, J = 7.6, 5.6 Hz), 4.99 (3H, br s), 4.55−4.46 (1H, m), 3.93 (1H, br s), 3.85 (2H, s), 3.73 (2H, s), 3.54−3.46 (2H, m), 3.46−3.38 (1H, m), 3.38−3.32 (2H, m), 3.19−3.13 (2H, m), 3.10−3.01 (1H, m), 2.84 (3H, s), 2.48−2.40 (1H, m), 2.17−2.10 (1H, m), 1.49−1.38 (13H, m), 1.24−1.14 (2H, m); δ_C (CD_3OD, 151 MHz) 173.3, 171.6, 161.8 (q, J = 36.8), 158.8, 148.0, 147.7, 143.6, 132.7, 127.7, 117.5 (q, J = 290.1), 80.9, 73.1, 72.1, 71.1, 56.7, 45.7, 45.1, 43.5, 40.3, 39.1, 30.1, 30.1, 28.7, 26.0, 24.5; HRMS (ESI): m/z calc'd for $C_{25}H_{42}N_5O_5$ $[MH]^+$ 492.3180, found 492.3189.

2-Amino-*N*-(2-((5-((*trans*-1-methyl-2-(pyridin-3-yl)-pyrrolidin-3-yl)methoxy)pentyl)amino)-2-oxoethyl)-acetamide, 9. A solution of carbamate **8** (60 mg, 0.0991 mmol) in 4 M HCl in dioxane/MeOH (5:3, 1.6 mL) was stirred at rt (1.5 h) before the solvent was removed in vacuo to give the title compound as a pale yellow oil (48 mg, 97%), δ_H (CD_3OD, 600 MHz) 9.36 (1H, s), 9.11 (1H, s), 9.06 (1H, s), 8.29 (1H, s), 4.75 (1H, s), 3.97 (1H, s), 3.93 (2H, s), 3.81 (2H, s), 3.74 (2H, t, J = 5.5 Hz), 3.67 (4H, q, J = 5.0 Hz), 3.61−3.55 (4H, m), 3.46 (1H, s), 3.35 (1H, s), 3.15 (3H, s), 2.89 (3H, s), 2.50 (1H, s), 2.11 (1H, s), 1.42 (2H, s), 1.38 (2H, s), 1.14 (2H, s); δ_C (CD_3OD, 151 MHz, mixture of rotamers and/or salt forms) 171.1, 168.0, 149.1, 144.4, 144.1, 135.1, 129.4, 73.5, 72.7, 72.4, 72.1, 71.8, 62.1, 56.9, 46.1, 43.8, 43.4, 41.7, 40.4, 39.4, 30.2, 26.0, 24.5; HRMS (ESI): m/z calc'd for $C_{20}H_{34}N_5O_3$ $[MH]^+$ 392.2656, found 392.2662.

5-Oxo-5-((3,5,7-tris(1-(*trans*-1-methyl-2-(pyridin-3-yl)-pyrrolidin-3-yl)-9,12,15-trioxo-2-oxa-8,11,14-triazahep-tadecan-17-yl)adamantan-1-yl)amino)pentanoic Acid, triAM1(Gly)$_2$, 10. PyBOP (21 mg, 0.0404 mmol) and Et_3N (23 μL, 0.161 mmol) were added to a solution of triacid **6** (5 mg, 0.0101 mmol) in DMF (200 μL) and the solution stirred at rt (5 min) before the addition of a solution of amine **9** (20 mg, 0.0404 mmol) in DMF (100 μL) and the solution stirred at rt (30 min). The reaction was quenched with H_2O (20 μL) and the reaction stirred at rt (5 min) before the solvent was removed in vacuo. Partial purification by preparative RP-HPLC (method 2, R_t = 32.2 min) followed by lyophilization gave the intermediate ester as a colorless oil. This was dissolved in MeOH (500 μL), 4 M aq. LiOH (100 μL) was added and the reaction stirred at rt (18 h). Purification by preparative RP-HPLC (method 2, R_t = 31.4 min) followed by lyophilization gave the title compound as a colorless oil (6.8 mg, 39%), δ_H (CD_3OD, 600 MHz) 8.85−8.80 (3H, m), 8.80−8.75 (3H, m), 8.31−8.19 (3H, m), 7.80−7.72 (3H, m), 4.41 (3H, br s), 3.96−3.88 (3H, m), 3.87−3.83 (9H, m), 3.50 (3H, dd, J = 9.8, 6.2 Hz), 3.46 (3H, dd, J = 9.8, 4.4 Hz), 3.42−3.32 (12H, m), 3.16 (6H, t, J = 7.0 Hz), 3.01 (3H, br s), 2.82 (9H, s), 2.46−2.38 (3H, m), 2.31 (2H, t, J = 7.5 Hz), 2.29−2.24 (6H, m), 2.20−2.12 (5H, m), 1.88−1.81 (2H, m), 1.69−1.61 (6H, m), 1.57−1.50 (6H, m), 1.49−1.40 (12H, m), 1.25−1.17 (9H, m), 1.14−1.08 (3H, m); δ_C (CD_3OD, 151 MHz) 177.5, 176.8, 174.8, 172.4, 171.5, 161.3 (q, J = 34.3 Hz), 150.3, 149.7, 140.8, 131.4, 126.8, 117.3 (J = 288.7 Hz), 73.4, 72.1, 71.0, 56.7, 54.8, 46.5, 45.6, 44.1, 43.6, 40.4, 39.5, 39.2, 37.0, 36.1, 34.1, 30.7, 30.2, 30.2, 26.1, 24.5, 22.5; HRMS (ESI): m/z calc'd for $C_{84}H_{130}N_{16}O_{15}$ $[MH_2]^{2+}$ 801.4945, found 801.4935.

1-(*trans*-1-Methyl-2-(pyridin-3-yl)pyrrolidin-3-yl)-9,12,15-trioxo-2-oxa-8,11,14-triazaheptadecan-19-oic Acid, AM1(Gly)$_2$, 11. PyBOP (40 mg, 0.0764 mmol) and Et_3N (32 μL, 0.229 mmol) were added to a solution of monomethylglutarate (10 μL, 0.0764 mmol) in DMF (250 μL) and the solution stirred at rt (5 min) before the addition of a solution of amine **9** (24 mg, 0.0510 mmol) in DMF (100 μL) and the solution stirred at rt (30 min). The reaction was quenched with H_2O (50 μL) and the reaction stirred at rt (10 min) before the solvent was removed in vacuo. The residue was dissolved in MeOH (1 mL), 4 M aq. LiOH (150 μL) was added, and the reaction stirred at rt (1.5 h). Purification by preparative RP-HPLC (method 2, R_t = 25.3 min) followed by lyophilization gave the title compound as a colorless oil (13 mg, 41%), δ_H (CD_3OD, 600 MHz) 8.88−8.82 (1H, m), 8.82−8.76 (1H, m), 8.35−8.24 (1H, m), 7.83−7.76 (1H, m), 4.43 (1H, br s), 3.94−3.86 (1H, m), 3.84 (2H, s), 3.84 (2H, s), 3.50 (1H, dd, J = 9.8, 6.2 Hz), 3.46 (1H, dd, J = 9.9, 4.3 Hz), 3.44−3.38 (1H, m), 3.38−3.31 (3H, m), 3.16 (2H, t, J = 7.1), 3.02 (1H, br s), 2.82 (3H, s), 2.47−2.38 (1H, m), 2.35 (4H, q, J = 7.3 Hz), 2.18−2.11 (1H, m), 1.94−1.88 (2H, m), 1.49−1.39 (4H, m), 1.24−1.16 (1H, m); δ_C (CD_3OD, 151 MHz) 176.8, 176.4,

dx.doi.org/10.1021/bc500016k | *Bioconjugate Chem.* 2014, 25, 593−600

172.5, 171.5, 161.8 (q, J = 38.3 Hz), 149.7, 149.2, 141.4, 131.7, 127.0, 117.6 (q, J = 290.7 Hz), 73.3, 72.1, 71.0, 56.7, 45.6, 44.1, 43.6, 40.3, 39.1, 35.7, 34.1, 30.1, 30.1, 26.0, 24.5, 21.9; HRMS (ESI): m/z calc'd for $C_{25}H_{40}N_5O_6$ $[MH]^+$ 506.2973, found 506.2976.

Conjugation of Haptens. A solution of hapten (150 mM), EDC.HCl (2.5−5.0 equiv) and sulfo-NHS (1.5−3 equiv) in 10% H_2O/DMF was agitated at rt until complete activation was observed by LCMS analysis (adding further EDC.HCl if necessary), whereupon the solvent was removed in vacuo. OVA or BSA (Pierce Imject, Thermo Fisher) (6.5−10 mg/mL in 100 mM MOPS-buffered saline (pH 7.2)) was added to the activated hapten AM1 (**1**) or AM1$(Gly)_2$ (**11**) (ca. 145 equiv for OVA, 215 equiv for BSA), triAM1 (**7**), or triAM1$(Gly)_2$ (**10**) (ca. 70 equiv for OVA, 100 equiv for BSA) and the solutions mixed (4 °C, 18−40 h), before the protein conjugates were dialyzed into PBS (pH 7.4) at 4 °C. OVA conjugates were used for immunization and BSA conjugates were used for ELISA plate coating.

BCA Assay for Determination of Protein Concentration. Protein concentrations were determined by a modification of Lowry's method,[28] using bicinchoninic acid (Pierce BCA Protein Assay Kit, Thermo Fisher), with BSA standards. Samples were incubated at 37 °C for 30 min before analysis on a Molecular Devices SpectraMax 250 plate reader at 562 nm.[29]

MALDI-TOF MS for Determination of Hapten Density. MALDI-TOF MS were performed on an Applied Biosystems Voyager-DE STR MS using sinapinic acid as the matrix. Average hapten density was estimated from the difference in mass of the conjugated carrier protein with its unconjugated counterpart taking into consideration the mass of the incorporated hapten unit (comparative MALDI-MS).[30]

Immunization. AM1-OVA, triAM1-OVA, triAM1$(Gly)_2$-OVA, and AM1$(Gly)_2$-OVA (100 μg) in PBS (100 μL, 1 mg/mL) formulated with Sigma Adjuvant System (SAS, 100 μL) were used to immunize groups of five to six BALB/c mice (8 weeks) via intraperitoneal injection on days 0, 14, and 35. Plasma was collected via retroorbital puncture on days 21, 42, and 56.

Immunologic Assays. *ELISA.* Production of anti-nicotine IgG was evaluated by ELISA. Costar 3690 microtiter plates were incubated with AM1-BSA in PBS (5 μg/mL, 25 μL) at 37 °C and the solution allowed to evaporate, before MeOH fixation. Nonspecific binding was blocked with 5% nonfat milk in PBS (30 min, 37 °C). Mouse plasma in 1% BSA (25 μL) was serially diluted across the plate before incubation in a moist chamber (1.5 h, 37 °C). After washing with dH_2O, peroxidase-conjugated donkey antimouse IgG (Jackson ImmunoResearch Laboratories, Inc.) was added and the plates incubated in a moist chamber (30 min, 37 °C). After further washing with dH_2O, plates were developed with the TMB substrate kit (Thermo Pierce) and the absorbance at 450 nm measured on a SpectraMax M2^e Molecular Devices microplate reader. Titers were calculated as the dilution corresponding to 50% of the maximum absorbance from a plot of the absorbance versus log(dilution) using GraphPad Prism 5.

Radioimmunoassay (RIA). Dissociation constants and antibody concentrations were determined using competitive RIA. Mouse plasma was pooled and diluted into 2% BSA, giving a concentration that was determined to bind ca. 40% L-(−)-[N-methyl-^{3}H]-nicotine tracer (20 000−30 000 dpm, 81.7 Ci/mmol (PerkinElmer, Boston, MA)). Diluted plasma (50−75 μL) and nicotine tracer (50−75 μL) in PBS were added to the sample chamber of a 5 kDa MWCO 96-well Equilibrium Dialyzer (Harvard Apparatus), and unlabeled (−)-nicotine (100−150 μL) at varying concentrations in 1% BSA was added to the buffer chamber. After equilibration on a plate rotator (Harvard Apparatus) at rt (22−26 h), a sample from each chamber (50−75 μL) was diluted into Ecolite(+) liquid scintillation cocktail (5 mL, MP Biomedicals) and the radioactivity measured using a Beckman LS 6500 Scintillation Counter. K_ds and antibody concentrations were calculated according to Müller.[31]

■ ASSOCIATED CONTENT

Ⓢ Supporting Information

Additional figures showing antibody titers at 21, 42, and 56 days, RIA-generated binding curves, NMR, and MALDI-TOF spectra. This material is available free of charge via the Internet at http://pubs.acs.org.

■ AUTHOR INFORMATION

Corresponding Author

*E-mail: kdjanda@scripps.edu, phone: (858) 784-2515, fax: (858) 784-2595.

Notes

The authors declare no competing financial interest.

■ ACKNOWLEDGMENTS

This work was funded by the Tobacco-Related Disease Research Program (TRDRP) grant no. 20XT-0156, the National Institutes of Health grant no. R01-DA026625 and the National Institute on Drug Abuse grant no. DA 08590. The authors acknowledge Dr. Amira Moreno, Dr. Jonathan Lockner, and Paul Bremer for helpful discussions.

■ ABBREVIATIONS

BCA, bicinchoninic acid assay; BCR, B cell receptor; BSA, bovine serum albumin; calc'd, calculated; dH_2O, deionized water; DMF, dimethylformamide; EDC, 1-ethyl-3-(3-dimethylaminopropyl)carbodiimide; ELISA, enzyme-linked immunosorbent assay; ESI, electrospray ionization; HOAt, 1-hydroxy-7-azabenzotriazole; HRMS, high-resolution mass spectrometry; Ig, immunoglobulin; K_d, dissociation constant; KLH, keyhole limpet hemocyanin; LCMS, liquid chromatography mass spectrometry; MALDI-TOF MS, matrix-assisted laser desorption/ionization time-of-flight mass spectrometry; MAP, multiple antigenic peptide; MHC, major histocompatibility complex; MOPS, 3-(N-morpholino)propanesulfonic acid; MWCO, molecular weight cutoff; NHS, N-hydroxysuccinimide; NMR, nuclear magnetic resonance; OVA, ovalbumin; PBS, phosphate-buffered saline; PyBOP, benzotriazol-1-yl-oxytripyrrolidinophosphonium hexafluorophosphate; RAFT, regioselectively addressable functionalized template; RIA, radioimmunoassay; RP-HPLC, reversed-phase high-performance liquid chromatography; SAS, Sigma Adjuvant System; SEM, standard error of the mean; TFA, trifluoroacetic acid; TLC, thin layer chromatography; TMB, 3,3′,5,5′-tetramethylbenzidine; UV, ultraviolet

■ REFERENCES

(1) World Health Organization, WHO Report on the Global Tobacco Epidemic, 2011: Warning about the Dangers of Tobacco.

(2) Hatsukami, D. K., Stead, L. F., and Gupta, P. C. (2008) Tobacco addiction. *The Lancet 371*, 2027−2038.
(3) Cornuz, J., Zwahlen, S., Jungi, W. F., Osterwalder, J., Klingler, K., van Melle, G., Bangala, Y., Guessous, I., Müller, P., Willers, J., Maurer, P., Bachmann, M. F., and Cerny, T. (2008) A vaccine against nicotine for smoking cessation: a randomized controlled trial. *PLoS ONE 3*, e2547.
(4) Hatsukami, D. K., Jorenby, D. E., Gonzales, D., Rigotti, N. A., Glover, E. D., Oncken, C. A., Tashkin, D. P., Reus, V. I., Akhavain, R. C., Fahim, R. E. F., Kessler, P. D., Niknian, M., Kalnik, M. W., and Rennard, S. I. (2011) Immunogenicity and smoking-cessation outcomes for a novel nicotine immunotherapeutic. *Clin. Pharmacol. Ther. 89*, 392−399.
(5) Janeway, C. A., Travers, P., Walport, M., and Shlomchik, M. J. (2001) Chapter 9. The Humoral Immune Response; B-cell Activation by armed helper T cells, in *Immunobiology: The Immune System in Health and Disease*, Garland Science, New York.
(6) Marco, M.-P., Gee, S., and Hammock, B. D. (1995) Immunochemical techniques for environmental analysis II. Antibody production and immunoassay development. *TrAC-Trends Anal. Chem. 14*, 415−425.
(7) Dintzis, H. M., Dintzis, R. Z., and Vogelstein, B. (1976) Molecular determinants of immunogenicity: the immunon model of immune response. *Proc. Natl. Acad. Sci. U.S.A. 73*, 3671−3675.
(8) Peri, F. (2013) Clustered carbohydrates in synthetic vaccines. *Chem. Soc. Rev. 42*, 4543−4556.
(9) Buskas, T., Thompson, P., and Boons, G.-J. (2009) Immunotherapy for cancer: synthetic carbohydrate-based vaccines. *Chem. Commun.*, 5335−5349.
(10) Dumy, P., Eggleston, I. M., Cervigni, S., Sila, U., Sun, X., and Mutter, M. (1995) A convenient synthesis of cyclic peptides as regioselectively addressable functionalized templates (RAFT). *Tetrahedron Lett. 36*, 1255−1258.
(11) Grigalevicius, S., Chierici, S., Renaudet, O., Lo-Man, R., Dériaud, E., Leclerc, C., and Dumy, P. (2005) Chemoselective assembly and immunological evaluation of multiepitopic glycoconjugates bearing clustered Tn antigen as synthetic anticancer vaccines. *Bioconjugate Chem. 16*, 1149−1159.
(12) Tam, J. P. (1988) Synthetic peptide vaccine design: synthesis and properties of a high-density multiple antigenic peptide system. *Proc. Natl. Acad. Sci. U.S.A. 85*, 5409−5413.
(13) Duryee, M. J., Bevins, R. A., Reichel, C. M., Murray, J. E., Dong, Y., Thiele, G. M., and Sanderson, S. D. (2009) Immune responses to methamphetamine by active immunization with peptide-based, molecular adjuvant-containing vaccines. *Vaccine 27*, 2981−2988.
(14) Moreno, A. Y., Azar, M. R., Warren, N. A., Dickerson, T. J., Koob, G. F., and Janda, K. D. (2010) A critical evaluation of a nicotine vaccine within a self-administration behavioral model. *Mol. Pharmaceutics 7*, 431−441.
(15) Janda, K. D. (2011) Nicotine haptens, immunoconjugates and their uses. WO 031327 (A2).
(16) Lockner, J. W., Ho, S. O., McCague, K. C., Chiang, S. M., Do, T. Q., Fujii, G., and Janda, K. D. (2013) Enhancing nicotine vaccine immunogenicity with liposomes. *Bioorg. Med. Chem. Lett. 23*, 975−978.
(17) Pryde, D. C., Jones, L. H., Gervais, D. P., Stead, D. R., Blakemore, D. C., Selby, M. D., Brown, A. D., Coe, J. W., Badland, M., Beal, D. M., Glen, R., Wharton, Y., Miller, G. J., White, P., Zhang, N., Benoit, M., Robertson, K., Merson, J. R., Davis, H. L., and McCluskie, M. J. (2013) Selection of a novel anti-nicotine vaccine: influence of antigen design on antibody function in mice. *PLoS ONE 8*, e76557.
(18) Zapotoczny, S., Biedroń, R., Marcinkiewicz, J., and Nowakowska, M. (2012) Atomic force microscopy−based molecular studies on the recognition of immunogenic chlorinated ovalbumin by macrophage receptors. *J. Mol. Recognit. 25*, 82−88.
(19) Boyaka, P. N., Ohmura, M., Fujihashi, K., Koga, T., Yamamoto, M., Kweon, M.-N., Takeda, Y., Jackson, R. J., Kiyono, H., Yuki, Y., and McGhee, J. R. (2003) Chimeras of labile toxin one and cholera toxin retain mucosal adjuvanticity and direct Th cell subsets via their B subunit. *J. Immunol. 170*, 454−462.
(20) Fleck, C., Franzmann, E., Claes, D., Rickert, A., and Maison, W. (2013) Synthesis of functionalized adamantane derivatives: (3 + 1)-scaffolds for applications in medicinal and material chemistry. *Synthesis 45*, 1452−1461.
(21) Lamoureux, G., and Artavia, G. (2010) Use of the adamantane structure in medicinal chemistry. *Curr. Med. Chem. 17*, 2967−2978.
(22) Still, W. C., Kahn, M., and Mitra, A. (1978) Rapid chromatographic technique for preparative separations with moderate resolution. *J. Org. Chem. 43*, 2923−2925.
(23) Cushman, M., and Castagnoli, N. (1972) Synthesis of trans-3′-methylnicotine. *J. Org. Chem. 37*, 1268−1271.
(24) Delimarskii, R. E., Rodionov, V. N., and Yurchenko, A. G. (1988) Preparative synthesis of 1,3,5-tribromoadamantane. *Ukr. Khim. Zh. 54*, 437−438.
(25) Baum, K., Archibald, T. G., and Malik, A. A. (1991) Ethynyl adamantane derivatives and methods of polymerization thereof. U. S. Patent 5017734 (A).
(26) Malik, A. A., Archibald, T. G., Baum, K., and Unroe, M. R. (1992) Thermally stable polymers based on acetylene-terminated adamantanes. *J. Polym. Sci., Part A: Polym. Chem. 30*, 1747−1754.
(27) Maison, W., Frangioni, J. V., and Pannier, N. (2004) Synthesis of rigid multivalent scaffolds based on adamantane. *Org. Lett. 6*, 4567−4569.
(28) Lowry, O. H., Rosebrough, N. J., Farr, A. L., and Randall, R. J. (1951) Protein measurement with the Folin phenol reagent. *J. Biol. Chem. 193*, 265−275.
(29) Smith, P. K., Krohn, R. I., Hermanson, G. T., Mallia, A. K., Gartner, F. H., Provenzano, M. D., Fujimoto, E. K., Goeke, N. M., Olson, B. J., and Klenk, D. C. (1985) Measurement of protein using bicinchoninic acid. *Anal. Biochem. 150*, 76−85.
(30) Wengatz, I., Schmid, R. D., Kreißig, S., Wittmann, C., Hock, B., Ingendoh, A., and Hillenkamp, F. (1992) Determination of the hapten density of immuno-conjugates by matrix-assisted UV laser desorption/ionization mass spectrometry. *Anal. Lett. 25*, 1983−1997.
(31) Müller, R. (1983) Determination of affinity and specificity of anti-hapten antibodies by competitive radioimmunoassay. *Methods Enzymol. 92*, 589−601.
(32) Pravetoni, M., Keyler, D. E., Pidaparthi, R. R., Carroll, F. I., Runyon, S. P., Murtaugh, M. P., Earley, C. A., and Pentel, P. R. (2012) Structurally distinct nicotine immunogens elicit antibodies with non-overlapping specificities. *Biochem. Pharmacol. 83*, 543−550.
(33) Pravetoni, M., Naour, M. L., Harmon, T. M., Tucker, A. M., Portoghese, P. S., and Pentel, P. R. (2012) An oxycodone conjugate vaccine elicits drug-specific antibodies that reduce oxycodone distribution to brain and hot-plate analgesia. *J. Pharmacol. Exp. Ther. 341*, 225−232.
(34) Cornish, K. E., Harris, A. C., LeSage, M. G., Keyler, D. E., Burroughs, D., Earley, C., and Pentel, P. R. (2011) Combined active and passive immunization against nicotine: Minimizing monoclonal antibody requirements using a target antibody concentration strategy. *Int. Immunopharmacol. 11*, 1809−1815.